UFSM

CIÊNCIA e NATURA

ISSN 2179-460X
OPEN ACCESS

Ci. e Nat., Santa Maria, e89084, v. 48, 2026 • https://doi.org/10.5902/2179460X89084
Submitted: 10/05/2024 • Approved: 05/21/2025 • Published: 07/01/2026

Environment

Photocatalytic degradation and phytotoxicity assessment of diclofenac and paracetamol using exfoliated g-C_3N_4/Nb_2O_5 under sunlight

Degradação fotocatalítica e avaliação da fitotoxicidade de diclofenaco e paracetamol usando g-C_3N_4/Nb_2O_5 esfoliado sob luz solar

Julia Mendes[I], José André Ferreira Batista[I], Maria Carolina Gomes Silva e Silva[I], Willian Cézar Nadaleti[I], Cátia Fernandes Leite[I], Priscila Martta Rodrigues[II], Cícero Coelho de Escobar[I]

[I] Universidade Federal de Pelotas, Pelotas, RS, Brasil
[II] Universidade do Vale do Rio dos Sinos, RS, Brasil

ABSTRACT

This study evaluated the effectiveness of the photodegradation process under artificial sunlight irradiation for two pharmaceutical compounds, paracetamol and diclofenac, using g-C_3N_4-based photocatalysts, and investigated the phytotoxic potential (*Lactuca sativa* and *Cucumis sativus*) of the generated products. Four photocatalysts were evaluated (g-C_3N_4, g-C_3N_4/Nb_2O_5, exfoliated g-C_3N_4, and exfoliated g-C_3N_4/Nb_2O_5). For cucumber seeds, photolysis was sufficient to maintain adequate phytotoxicity, ensuring germination indices above 80% for both drugs. In contrast, for lettuce seeds, photolysis did not show the same performance, highlighting the need for heterogeneous photocatalysis. Regarding degradation, the average degradation rate of the four photocatalysts was higher (71.5%) for diclofenac, being 3.3 times greater than for paracetamol. Compared to bulk g-C_3N_4, the exfoliated g-C_3N_4/Nb_2O_5 photocatalyst was the most efficient, exhibiting degradation kinetic values 1.5 and 13.8 times higher for diclofenac and paracetamol, respectively. The results also indicate that the exfoliation step and the incorporation of niobium increase the surface area values, which ranged from 11 to 61 m²/g.

Keywords: Graphitic carbon nitride; Pharmaceuticals; Advanced oxidative processes

RESUMO

Este estudo avaliou a eficácia do processo de fotodegradação sob irradiação de luz solar artificial para dois compostos farmacêuticos, paracetamol e diclofenaco, utilizando fotocatalisadores à base de g-C_3N_4, além de investigar o potencial fitotóxico (*Lactuca sativa* e *Cucumis sativus*) dos produtos gerados. Quatro fotocatalisadores foram avaliados (g-C_3N_4, g-C3N_4/Nb_2O_5, g-C_3N_4-esfoliado e g-C_3N_4/Nb_2O_5-esfoliado). Para as

sementes de pepino, a fotólise foi suficiente para manter uma fitotoxicidade adequada, garantindo Índices de Germinação acima de 80% para ambos os fármacos. Por outro lado, para as sementes de alface, a fotólise não apresentou o mesmo desempenho, destacando a necessidade da fotocatálise heterogênea. Em relação à degradação, a taxa média de degradação dos quatro fotocatalisadores foi maior (71,5%) para o diclofenaco, sendo 3,3 vezes maior que a do paracetamol. Comparando com o g-C_3N_4 na forma bulk, o fotocatalisador g-C_3N_4/Nb_2O_5-esfoliado apresentou valores de cinética de degradação 1,5 e 13,8 vezes maiores para diclofenaco e paracetamol, respectivamente. Os resultados também indicam que a etapa de esfoliação e a incorporação de nióbio aumentam os valores de áreas superficial, que variaram de 11 a 61 m^2/g.

Palavras-chave: Nitreto de carbono grafítico; Fármacos; Processos oxidativos avançados

1 INTRODUCTION

Recent literature highlights growing concerns about persistent organic pollutants (Puri et al., 2023), among which pharmaceutical compounds in wastewater stand out. The global consumption of pharmaceuticals has risen, along with their detection in wastewater, surface water, and even water intended for human consumption (Zhou et al., 2019). These compounds include analgesics, anti-inflammatories, antibiotics, antiepileptics, beta-blockers, blood lipid regulators, contrast media, hormones, antidepressants, and anxiolytics.

While conventional wastewater treatments effectively transfer contaminants from the liquid to the solid phase, they do not ensure complete degradation (Wang et al., 2022). For the effective removal of these recalcitrant pollutants, they must be mineralized into harmless compounds like water, carbon dioxide, and oxidized inorganic anions. Advanced Oxidative Processes (AOPs), particularly heterogeneous photocatalysis, are recognized as efficient methods for degrading such organic pollutants (Wang et al., 2022). However, widely studied photocatalysts like TiO_2 and ZnO require ultraviolet light due to their wide band gaps (Mathew et al., 2020; Moreno et al., 2022), prompting research into catalysts that are active under visible light (Friedmann, 2022; Mathew et al., 2020; Moreno et al., 2022).

Graphitic carbon nitride (g-C_3N_4), a metal-free photocatalyst, has gained attention for its easy synthesis, favorable semiconductor properties, and thermal and

photochemical stability (Liu et al., 2020; Wang et al., 2022). Unlike TiO_2, g-C_3N_4 has a moderate band gap, allowing it to absorb visible light in the 450-460 nm range (Wang et al., 2022). However, its practical application faces challenges, such as low surface area, poor electronic conductivity, and rapid recombination of electron-hole pairs generated by light (Luo et al., 2023; Wang et al., 2022).

Several strategies have been explored to overcome these limitations, such as exfoliation and the creation of heterojunctions, which improve light absorption and charge separation. Exfoliating bulk g-C_3N_4 into two-dimensional (2D) structures increases its surface area, allowing greater exposure of active sites and enhancing photocatalytic activity (Smýkalová et al., 2019; Zhang et al., 2022). This process also improves the dispersion of photoinduced charge carriers, reducing recombination and boosting photocatalytic efficiency (Zhang et al., 2022). Several exfoliation methods have been investigated, including thermal, chemical, and physical processes (ultrasound-assisted), with thermal processes generally providing better performance (Abega et al., 2023; Zhang et al., 2022).

Doping g-C_3N_4 with non-metallic elements or integrating it with other semiconductors, like niobium pentoxide (Nb_2O_5), can further enhance its properties. Nb_2O_5, a wide-bandgap semiconductor known for its stability and excellent charge transport, forms a heterojunction with g-C_3N_4 that facilitates better electron-hole separation, improving photocatalytic efficiency (Carvalho et al., 2017; da Silva et al., 2017).

Another important aspect is that, while photocatalysis effectively degrades pharmaceuticals, it may also provide a viable approach for utilizing the resultant byproducts, which could be used for water reuse in irrigation or as ingredients in liquid fertilizers (Ravindran et al., 2016). However, there is a gap in the current understanding of the phytotoxicity associated with pharmaceutical byproducts formed through reactions with g-C_3N_4-based photocatalysts (Batista et al., 2023) , which this study also seeks to address.

Considering the above remarks, it is reasonable to assume that the introduction of Nb modifies the electronic structure of exfoliated g-C_3N_4, which could enhance light

absorption in the visible range and further improve its oxidative potential, making it more effective in degrading persistent organic pollutants like pharmaceuticals. In light of these considerations, this study aims to evaluate the effectiveness of the photodegradation process under artificial sunlight irradiation for two pharmaceutical compounds, paracetamol (analgesic) and diclofenac (anti-inflammatory), using thermal exfoliated g-C_3N_4-based photocatalysts containing niobium, while also investigating the phytotoxic potential of the generated products. In this sense, the novelty of this work lies in demonstrating that the concomitant presence of exfoliation and niobium in g-C_3N_4-based photocatalysts should enhance the degradation efficiency of diclofenac and ibuprofen. To the best of our knowledge, no studies have yet described a comparison of these two characteristics, particularly in comparison with the bulk counterparts (non-exfoliated) of these same photocatalysts.

2 MATERIALS AND METHODS

2.1 Chemical reagents

Sodium diclofenac (DCF, ≥ 99%) and hydrochloric acid (HCl, 37%) were supplied by Sigma-Aldrich. Niobium pentachloride ($NbCl_5$, ≥99.5%) was obtained from the Brazilian Company of Mining and Metallurgy (CBMM, Brazil). Melamine (99.0%) and ammonium chloride (NH_4Cl) were commercially available chemicals obtained from Merck Company and used without further purification.

2.2 Preparation of photocatalysts and characterization

Initially, bulk g-C_3N_4 was synthesized using 5 g of melamine as the raw material. The precursor was placed in a muffle furnace at a temperature of 500°C for 4 hours using a covered alumina crucible. Next, the obtained material was calcined again in the muffle furnace (500°C for 2 hours) to form the exfoliated photocatalyst (g-C_3N_4-E). The production of bulk g-C_3N_4/Nb_2O_5 began by initially mixing 10 mL of ammonia solution

with 0.2 g of $NbCl_5$ and 5 g of melamine. The mixture was then acidified with 0.5 M HCl, magnetically stirred for 2 hours, then dried and subsequently subjected to calcination (500°C for 4 hours). For the production of g-C_3N_4/Nb_2O_5-E, the previous material was calcined again at 500°C for 2 hours. The preparation of the four photocatalysts is summarized in the flowchart shown in Figure 1.

Figure 1 – Schematic diagram of the fabricated photocatalysts

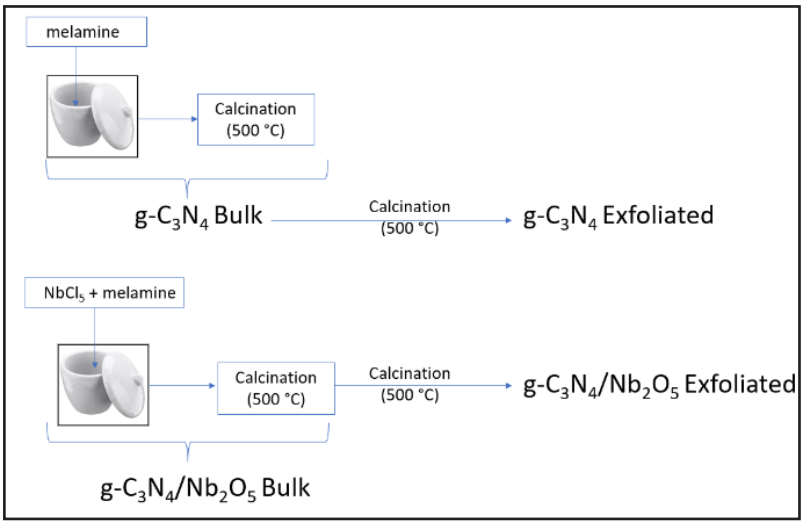

Source: Authors (2024)

The determination of specific surface area utilized the Brunauer-Emmett-Teller (BET) method at a temperature of −196 °C, operating within the partial pressure range of $0.2 < P/P_0 < 0.9$, employing a surface area analyzer (Gemini 2375 Micromeritics, Norcross, USA). Prior to each measurement, the samples underwent preheating at 110 °C for 14 hours under vacuum conditions.

The solid samples (photocatalysts) underwent ultraviolet-visible analysis, wherein approximately 0.05 g was dispersed onto an analysis cell. These samples were examined using a Varian spectrophotometer Cary 100 (Santa Clara, USA) equipped with a DRA-CA-301 accessory (Labsphere) for diffuse reflectance analysis (DRS). Spectra were acquired at room temperature using BaSO4 as a reference, within the spectral range of 200 to 800 nm. The absorbance results were utilized in Tauc's equation for calculating the band gap, following Equation 1.

$$\alpha h\nu = A(h\nu - E_g)^n \quad (1)$$

Where:
α - absorption coefficient of the material;
hν - energy of the incident photon;
E_g - material's band gap;
A - constant related to the probability of optical transition;
n - exponent that depends on the type of optical transition (typically assumed values range between 1/2 and 2).

To determine the value of Eg from this equation, it's necessary to plot a graph of $(\alpha h\nu)^2$ versus hν. From this graph, it's possible to extrapolate the intersection with the abscissa axis, which corresponds to the band gap value.

2.3 Heterogeneous photocatalysis

The degradation experiments were performed within a batch reactor utilizing a 300 W lamp (OSRAM), which replicate the solar spectrum (Ines et al., 2019; Osram, 2016). All assessments were conducted with the lamp positioned 25 cm away from the drug solution's surface (either paracetamol or diclofenac). To uphold the reactor's temperature at 30°C, a circulating water system was employed. Tests were conducted at the drugs' inherent pH levels. Throughout the reaction, radiation intensity remained constant at 40 $W.m^{-2}$ for UV-A and 245 $W.m^{-2}$ for visible light, assessed via a radiometer (Delta Ohm, HD 2302.0).

The tests were carried out with 600 mg/L of the photocatalyst in a bath reactor under continuous air flow (6.5 $mL.\ s^{-1}$) with 250 mL of a pharmaceutical solution (20 mg/L). The selection of this catalyst amount is based on prior studies that have demonstrated its efficacy in achieving high percentages of diclofenac removal. Equilibrium (Liu et al., 2019; Papamichail et al., 2023).

The results of the photocatalytic tests were evaluated in two stages under magnetic stirring (around 400 rpm) as follows: (i) one hour with the lamp off (adsorption-desorption equilibrium) and (ii) two hours with the lamp on (degradation).

Subsequently, the lamp was activated. Aliquots were then taken and filtered through a 0.22 µm Millipore filter. The final concentration was determined by UV-Vis molecular absorption spectroscopy using a Varian Cary 100 spectrophotometer. Degradation was estimated from the calibration curves for each drug. All tests were performed in triplicates. The degradation after the tests was estimated according to Equation 2.

$$\text{Degradation (\%)} = \frac{C_0 - C}{C_0} \times 100\% \quad (2)$$

In which C_0 is he initial drug concentration (20 mg/L) after 30 min of dark adsorption and C is the final concentration. The selection of this drug concentration is based on several other studies that investigated the extent of degradation of pharmaceutical compounds in artificial pharmaceutical solutions that can be analyzed using UV-VIS spectroscopy (da Silva et al., 2017; Hernández-Uresti et al., 2016; Jiménez-Salcedo et al., 2021; Lara-Pérez et al., 2020). The photocatalytic reactions were conducted at their natural pH, except for the investigation of pH influence, in which the paracetamol solutions were adjusted using 1 M NaOH and HCl.

The value of the kinetic constant was calculated based on a pseudo-first-order model, according to Equation 3.

$$\ln\left(\frac{C_0}{c}\right) = kt \quad (3)$$

Where:
C_0 - initial concentration (mg/L);
C - final concentration (mg/L);
t - time of reaction (min);
k - kinetic constant (min^{-1}).

The electrical energy per order (EEO) is known as the number of kilowatts of electrical energy required for decreasing the pollutant's concentration by one order of magnitude (90%) in 1.0 m³ of the polluted water, and it was calculated according to Equation 3 (Pizzichetti et al., 2023).

$$EEO = \frac{38.38.P}{V.k} \quad (4)$$

Where:
P - rated power or energy input (kW) of the lamp system;
V - volume (m^3) of solution treated in the photoreactor;
k - kinetic constant (min^{-1}).

Total organic (TOC) was monitored by a TOC-V_{SCH} Shimadzu carbon analyzer, for samples after 120 of photocatalysis. To assess the reusability of the g-C_3N_4 catalyst, consecutive cycles of degradation were performed. After each cycle, the solution underwent centrifugation to separate the catalyst, allowing an aliquot of the supernatant to be collected for analysis while ensuring a consistent catalyst quantity in all cycles. The required volume of drug solution was then added to restore the initial concentration conditions and initiate the next cycle.

For the radical trapping assays, isopropanol (IPA), ethylenediaminetetraacetic acid (EDTA), and benzoquinone (BQ) were utilized as selective scavengers for hydroxyl radicals (•OH), photogenerated holes (h^+), and superoxide anion radicals ($•O_2^-$), respectively. The experimental protocol was analogous to that employed in the photocatalytic performance evaluation, with the specific modification of incorporating 1 mmol of each scavenger into the reaction system.

2.4 Phytotoxicity essays

The phytotoxicological assays were conducted using the methodology described by (Zucconi, 1981) using seeds from two distinct plant species: Summer Regina lettuce (*Lactuca sativa*) and Long Green cucumber (*Cucumis sativus*). The relative root growth (RRG) was assessed using a digital caliper with 0.1 mm precision, alongside the relative seed germination (RSG), considering seeds as germinated if they exhibited a root length exceeding 1 mm, generating germination indices (GI). All seeds utilized were from the Isla® brand, free from pesticide treatment. The seed germination tests were conducted in triplicate.

Ten cucumber seeds and ten lettuce seeds were individually positioned in 9 cm diameter Petri dishes for each trial. These dishes held a layer of filter paper and 5 mL of effluent, while the control sample used distilled water. The prepared plates were then kept in the dark at 25°C for 72 hours. Following this incubation period, the number of germinated seeds was tallied, and the length of their roots was recorded. Using these measurements, Equation 5 was employed to compute the Germination Index (GI).

$$GI = \frac{(RSG) \times (RRG)}{\overline{RSG} \times \overline{RRG}} \times 100\% \quad (5)$$

Where:
RSG - number of germinated seeds in the sample plate;
RRG - root growth in the sample plate;
$\overline{RSG\,RSG}$ - average of germinated seeds in the control;
$\overline{RRGRRG}$ - average root growth in the control plates.

2.5 Statistical analysis

All results are expressed as mean values of triplicate experiments to ensure reproducibility and statistical reliability. Prior to conducting comparative analyses, the normality of the data distribution was evaluated using the Shapiro-Wilk test, which confirmed that the data met the assumptions required for parametric testing. Given the confirmation of normality, a one-way analysis of variance (ANOVA) was applied to investigate potential differences among group means. ANOVA is a robust statistical method well-suited for comparing three or more independent groups while minimizing the risk of Type I errors. When statistically significant differences were identified by ANOVA ($p \leq 0.05$), post hoc tests were performed to determine which specific groups differed from one another. For this purpose, both the Least Significant Difference (LSD) method and the Tukey Honestly Significant Difference (HSD) test were employed. The LSD test allows for pairwise comparisons with increased sensitivity, while the Tukey HSD test provides a more conservative approach by adjusting for multiple comparisons

(i.e., when more than three groups are involved), offering greater control over the family-wise error rate. In cases where only two groups were compared, the student's t-test was used to assess whether the differences between means were statistically significant. This test is appropriate for evaluating differences between two independent samples when normality is confirmed. All statistical analyses were conducted using a significance threshold of $p \leq 0.05$.

3 RESULTS AND DISCUSSION

3.1 Heterogeneous photocatalysis

Table 1 shows the results related to the surface area, band gap energy, and kinetic constants derived from the degradation of diclofenac and paracetamol. BET analysis revealed that the specific surface area of g-C_3N_4 was 11 m²/g, which is consistent with previously reported values for materials synthesized using melamine as a precursor (Jiang et al., 2017; Papamichail et al., 2023). The surface area of the other samples showed noticeable increases. This can be attributed both to the effect of the additional calcination process (exfoliation) or the presence of niobium, which indicates the effective formation of composite materials. Previous studies have reported that g-C_3N_4/Nb_2O_5 heterostructures exhibit surface areas ranging from 23 to 134 m²/g (Carvalho et al., 2017; Hong et al., 2016), suggesting that material preparation variables—such as calcination temperature, the Nb_2O_5 to g-C_3N_4 ratio, and the use of either Teflon-lined hydrothermal synthesis reactors or crucibles heated in muffle furnaces—can significantly influence the textural properties of the resulting material.

The band gap values were calculated in the range of 2.6 to 3.1 eV, consistent with other authors in the literature (Jiang et al., 2017; Zheng et al., 2016). It is important to note that materials with smaller band gaps can respond to visible light more effectively, as they require less energy to excite electrons from

the valence band to the conduction band. This makes them more suitable for photocatalytic applications under visible light, which is a key feature for energy-efficient processes like solar-driven catalysis. In contrast, materials with a larger band gap might only absorb UV light, which constitutes a smaller portion of the solar spectrum. Thus, the band gap range found for the photocatalysts in this study indicates their capacity to respond to visible light—a crucial characteristic for photocatalysts (Wang et al., 2022). This aspect is also important considering that the lamp used in the photocatalysis tests of this study emits a spectrum that simulates the wavelengths of sunlight (Ines et al., 2019).

Table 1 – Surface area (S_{BET}), band gap energy (E_g) and kinetic constant (k)

Photocatalyst	S_{BET} (m^2g^{-1})	E_g (eV)	k (min^{-1}) from diclofenac	k (min^{-1}) from paracetamol
g-C^3N^4	11+/-1.2	3.1	0.0097+/-0.0006	0.0004+/-0.00003
g-C^3N^4-E	22+/-2.0	2.7	0.0105+/-0.0011	0.0021+/-0.0002
g-C^3N^4/Nb^2O^5	27+/-1.7	2.9	0.0082+/-0.0005	0.0011+/-0.00032
g-C^3N^4/ Nb^2O^5-E	61 +/-3.7	2.6	0.0151+/-0.0001	0.0053+/-0.00041

Source: Authors (2024)

Experiments conducted under dark conditions revealed that the adsorption of the molecules was typically below 10%. The highest adsorption percentages were observed for g-C_3N_4/Nb_2O_5-E, with 9.7% for diclofenac and 8.3% for ibuprofen, and for g-C_3N_4-E, with 7.2% and 5.1%, respectively. These results suggest that, although the values are low, the exfoliation step slightly improves performance, as the bulk materials (g-C_3N_4 and g-C_3N_4/Nb_2O_5) showed adsorption values below 5% for both pharmaceuticals.

The degradation values during 120 minutes obtained for the different photocatalysis tests are shown in Figure 2. For comparison purposes, the performance of photolysis is also shown. For both drugs analyzed, photolysis showed the lowest degradation values. This result suggests that the action of artificial sunlight alone (in the absence of a photocatalyst) is incapable of achieving photodegradation of these drugs. Comparing the drugs, it can be seen that diclofenac was more extensively degraded

for all the four photocatalysts evaluated. After 120 min., the average degradation for diclofenac obtained by the four photocatalysts was 71.5%, equivalent to 3.3 times the average degradation value obtained for paracetamol.

Figure 2 – Effect of the photocatalyst on the photodegradation of diclofenac (a) and paracetamol (b) under simulated solar light (C_0= 20 mg/L; $C_{cat.}$ = 600 mg/L; pH_i (paracetamol) = 6.6 ± 0.18; pH_i (diclofenac) = 6.5 ± 0.11; irradiation = 40 W.m^{-2} UV-A, 245 W.m^{-2} VIS). The bars indicate the standard error

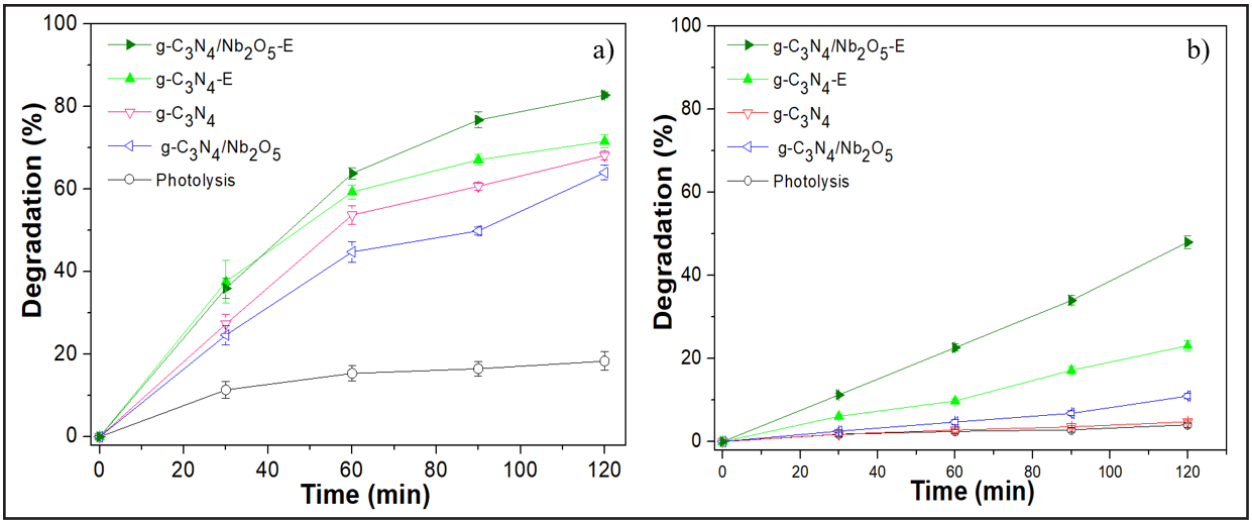

Source: Authors (2024)

For the degradation of diclofenac (Fig. 2a), it can be observed that all photocatalysts demonstrated degradation of the drug over the 120 minutes of reaction. It also can be seen that the exfoliated samples showed better results, reaching 82% and 71% degradation for the g-C_3N_4/Nb_2O_5-E and g-C_3N_4-E samples, respectively. These values are equivalent to 1.3 and 1.05 times higher compared to their bulk (non-exfoliated) counterparts, C_3N_4/Nb_2O_5 and g-C_3N_4, respectively.

For the degradation of paracetamol (Fig. 2b), the photocatalysts with the best performance were also the exfoliated ones, achieving 48% and 23% degradation with the g-C_3N_4/Nb_2O_5-E and g-C_3N_4-E samples, respectively. These values are approximately 4.7 times higher compared to their bulk counterparts.

The higher degradation rates observed for diclofenac compared to paracetamol can be primarily attributed to structural differences and chemical properties between the two molecules, which influence their susceptibility to photodegradation. Diclofenac exhibits a more conjugated aromatic structure and functional groups that are more prone to oxidation reactions, such as the secondary amine group and the carboxylic acid group. These features facilitate interactions with reactive species generated during photocatalysis, promoting its degradation. On the other hand, although paracetamol also possesses an aromatic ring, it has a simpler structure, with lower conjugation and relatively higher chemical stability against oxidative processes. Additionally, the phenolic bond in paracetamol may confer some resistance to degradation under certain photocatalytic conditions, especially when compared to more reactive compounds like diclofenac.

These differences have already been reported in the literature. Smykalová et al. (2019) observed superior performance in diclofenac degradation compared to paracetamol under photocatalysis with g-C_3N_4, with diclofenac showing a 77% degradation rate compared to 41% for paracetamol, under visible irradiation. Similar results were verified in the present study, reinforcing that the molecular characteristics of the target compounds are crucial determinants of their photocatalytic degradation efficiency. However, it is worth noting that Smykalová et al. (2019) did not explore the use of sunlight, which emits both UV and visible light, nor did they evaluate phytotoxic effects.

In comparison with the literature, the diclofenac degradation rates observed here were also similar to or lower than those reported in previous studies. However, it is important to note that direct comparisons between studies are often challenging due to variations in experimental conditions, such as initial contaminant concentrations, reaction times, light sources, and other parameters that significantly affect process efficiency. Despite these differences, some studies have reported that exfoliated g-C_3N_4 (250 mg/L) can degrade approximately 70% of diclofenac (10 mg/L)

over 6 hours under LED irradiation (Muelas-Ramos et al., 2021), and nearly 90% when using a 500 mg/L concentration of exfoliated g-C_3N_4 under a solar-simulated light source (300–800 nm) (Abega et al., 2023). Therefore, the diclofenac removal achieved in the present work using the best-performing photocatalyst (g-C_3N_4/Nb_2O_5-E, 83%) is in good agreement with the literature.

Regarding paracetamol, studies evaluating exfoliated g-C_3N_4 are scarce. SMYKALOVÁ et al. (2019) reported even lower degradation rates (41%) compared to the 48% observed in the present work with the best-performing material. Other authors have reported higher degradation efficiencies, such as 95% within just 60 minutes of visible light exposure (Hassan et al., 2024); however, the material used in those studies was markedly different, such as ZnO/g-C_3N_4 heterostructures operating via an S-scheme mechanism.

The effectiveness of the photocatalysts was further evaluated by measuring the kinetic rate constants throughout the reaction period, calculated using Equation 3. These values were derived from the average of three replicates from the photocatalytic experiments. In the case of diclofenac degradation, the kinetic constants in descending order were: g-C_3N_4/Nb_2O_5-E > g-C_3N_4-E > g-C_3N_4 > g-C_3N_4/Nb_2O_5, whereas for paracetamol, the descending order was: g-C_3N_4/Nb_2O_5-E > g-C_3N_4-E > g-C_3N_4/Nb_2O_5 > g-C_3N_4. (Table 1). In other words, the material that was simultaneously exfoliated and contains the presence of niobium (g-C_3N_4/Nb_2O_5-E) exhibited the best performance compared to the bulk g-C_3N_4 sample.

The Figure 3 illustrates whether there was an increase or decrease in the kinetic constant of the three catalysts (g-C_3N_4-E, g-C_3N_4/Nb_2O_5, and g-C_3N_4/Nb_2O_5-E/Nb_2O_5) compared to the bulk g-C_3N_4 sample. As can be seen, by dividing the kinetic constant obtained for each catalyst by that of bulk g-C_3N_4, a value greater than 1 indicates enhanced performance in favor of the exfoliated material or the one containing niobium. The comparison between g-C_3N_4/Nb_2O_5-E and bulk g-C_3N_4 revealed higher kinetic ratios for both diclofenac and paracetamol, with values of 1.5

and 13.8, respectively. Therefore, these results corroborate that the simultaneous presence of both the exfoliation process and niobium (g-C_3N_4/Nb_2O_5-E) enhances the removal performance of both pharmaceuticals.

Figure 3 – kinetic ratio for photocatalyst in comparison with bulk g-C_3N_4

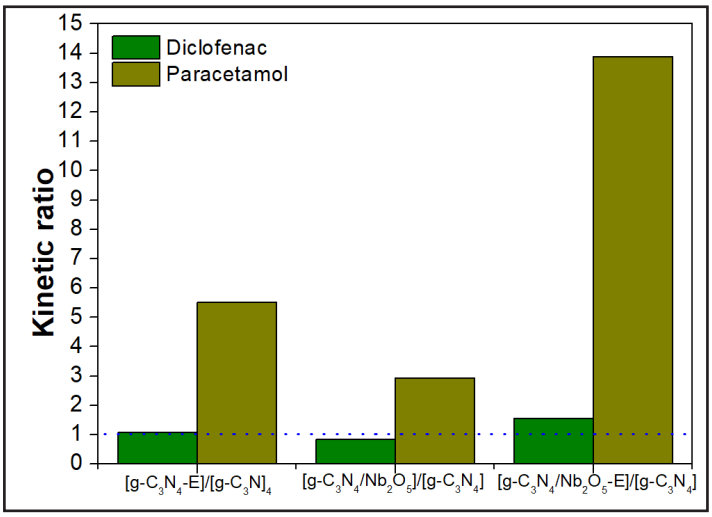

Source: Authors (2024)

For better comprehension of the results, the degradation efficiencies were compared using a mean difference test (ANOVA) in relation to the degradation achieved in 120 minutes. As shown in Table 2, most comparisons revealed statistical differences, with only three exceptions discussed as follows. First, the degradation between photolysis vs. g-C_3N_4 for paracetamol was not statistically different, suggesting that bulk g-C_3N_4 showed performance indistinguishable from photolysis. Second, for diclofenac degradation, there was no statistical difference between the photocatalysts g-C_3N_4 vs. g-C_3N_4-E, indicating that the exfoliation step did not improve the degradation efficiency for this drug. On the other hand, it is important to mention that a significant difference was found between these two photocatalysts for paracetamol degradation, suggesting that the exfoliation step may be beneficial for the removal of one drug but not necessarily for another. Third, only for diclofenac degradation, there was no significant difference between the pair g-C_3N_4 vs. g-C_3N_4/Nb_2O_5, suggesting that for the non-exfoliated samples, the performances are similar.

Table 2 – Tukey's test for the average removal values obtained between the pairs of photocatalysts, where * = P ≤ 0.05, ** = P ≤ 0.01, *** = P ≤ 0.001, **** = P ≤ 0.0001, and ns = statistically non-significant

Pairwaise comparison	Diclofenac	Paracetamol
Photolysis vs. g-C_3N_4	****	ns
Photolysis vs. g-C_3N_4-E	****	****
Photolysis vs. g-C_3N_4/Nb_2O_5	****	**
Photolysis vs. g-C_3N_4/Nb_2O_5-E	****	****
g-C_3N_4 vs. g-C_3N_4-E	ns	****
g-C_3N_4 vs. g-C_3N_4/Nb_2O_5	ns	**
g-C_3N_4 vs. g-C_3N_4/Nb_2O_5-E	***	****
g-C_3N_4-E vs. g-C_3N_4/Nb_2O_5	*	****
g-C_3N_4-E vs. g-C_3N_4/Nb_2O_5-E	**	****
g-C_3N_4/Nb_2O_5 vs. g-C_3N_4/Nb_2O_5-E	****	****

Source: Authors (2024)

By integrating the data from Table 2 with the degradation results (Figures 2 and 3), the superiority of the photocatalyst containing niobium and subjected to exfoliation (g-C_3N_4/Nb_2O_5-E) is further reinforced. This material exhibited the highest degradation efficiency, the largest BET surface area, and a suitable band gap energy (Eg), all indicating its enhanced photocatalytic performance. Moreover, two important characteristics of the studied materials must be highlighted. First, the extra calcination step, which ensures that g-C_3N_4 is exfoliated, can lead to an improvement in photocatalytic efficiency, especially for paracetamol. Second, the presence of niobium in the composition of the photocatalysts enhances the degradation efficiency of these pharmaceuticals. These two characteristics can be confirmed by observing that, in all comparisons made, the samples where both niobium and exfoliated process were present, (i.e., Nb_2O_5-E) photocatalyst showed statistically significant differences.

Exfoliated g-C_3N_4-based photocatalysts generally exhibit superior performance compared to their bulk counterparts, as recently reported in the

literature (Abega et al., 2023; Montalvo-Herrera et al., 2022). This enhancement is attributed to several key improvements introduced during the exfoliation process. The additional thermal treatment applied during exfoliation disrupts the stacked layered structure of bulk g-C_3N_4, producing thinner nanosheets with a significantly larger surface area. This morphological transformation increases the number of active sites available for photocatalytic reactions and enhances the material's dispersion in aqueous media. Moreover, exfoliation can induce modifications in the electronic structure, including slight shifts in the bandgap energy and more effective separation and migration of photogenerated charge carriers.

According to a study (Zhang et al., 2022), a comparison of several exfoliation methods—such as chemical, ultrasonic, and one-step thermal approaches—showed that the one-step method produced nanosheets with superior photocatalytic performance under visible light. In this approach, the precursor solution was placed in a sealed, lidded crucible to slow down the evaporation rate, similar to the method used in the present study. The resulting nanosheets exhibited a higher specific surface area, an optimized band gap, and enhanced charge separation efficiency, leading to bisphenol A degradation rate constants up to 6.5 times higher than those of bulk g-C_3N_4. In addition, a recent literature review also suggests that the presence of niobium may enhance the performance of g-C_3N_4-based photocatalysts (Jiang et al., 2020).

The TOC analysis (Figure 4) performed at the end of the 120-minute reaction for g-C_3N_4/Nb_2O_5-E revealed a difference in removal efficiency between the compounds. The TOC removal for diclofenac reached 76.6%, in agreement with reports in the literature (Torres-Pinto et al., 2023), and was 1.8 times higher than that observed for paracetamol, mirroring the degradation efficiency results (Fig. 2), and also indicating superior mineralization for diclofenac.

The comparison between UV-Vis and TOC results highlights the degradation by-products. The TOC data showed a higher mineralization efficiency for diclofenac (76.6%)

compared to paracetamol, which was consistent with the UV-Vis analysis. In addition, UV-Vis spectrum did not reveal significant degradation products for either drug.

Figure 4 – TOC removal obtained for diclofenac and paracetamol under simulated solar light using g-C_3N_4/Nb_2O_5-E (C_0= 20 mg/L; $C_{cat.}$ = 600 mg/L; pH_i (paracetamol) = 6.6 ± 0.18; pH_i (diclofenac) = 6.5 ± 0.11; irradiation = 40 W.m^{-2} UV-A, 245 W.m^{-2} VIS). The bars indicate the standard error

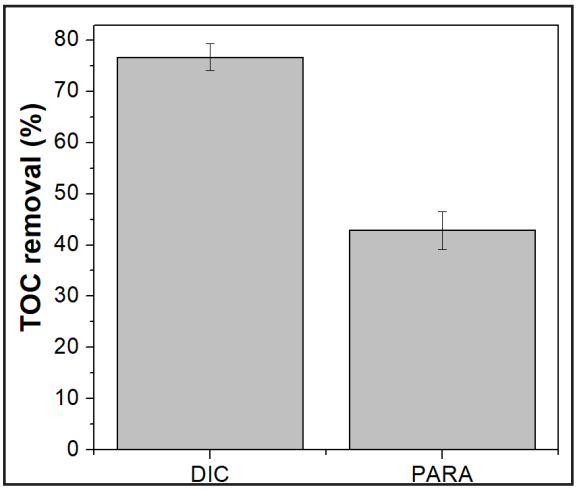

Source: Authors (2024)

The electrical energy per order (EEO) is defined as the electric energy in kWh required to reduce the concentration of a contaminant by one order of magnitude (90% removal) in 1 m^3 of water, and it is measured in batch operations, according to Equation 4, being useful for identifying the overall energy consumption. EEO was evaluated for the best material (g-C_3N_4/ Nb_2O_5-E), being 3 and 8.7 kWh/m^3 for degradation of diclofenac and of paracetamol, respectively. The results found are similar to others found in the literature aiming at the degradation of pharmaceuticals (Karimi et al., 2022; Sigcha-Pallo et al., 2022) using conventional photocatalysts such as TiO_2 and ZnO.

The higher specific surface area obtained for the g-C_3N_4/Nb_2O_5-E sample, as well as its lower band gap value, are consistent with the expectations generated by the characterization analyses. The larger surface area is favorable, as it is associated with improved contaminant degradation performance. Meanwhile,

the lower band gap indicates that the material can absorb visible light photons more efficiently, which is particularly relevant given that the lamp used in this study emits in this spectral range.

Considering that the g-C_3N_4/Nb_2O_5-E photocatalyst showed the most promising results, subsequent analyses of pH variation, reuse, and scavengers were limited to this material.

3.2 Influence of pH

Figure 5 – Effect of pH in degradation of diclofenac and paracetamol under simulated solar light after 120 min using g-C_3N_4/Nb_2O_5-E. The bars indicate the standard error

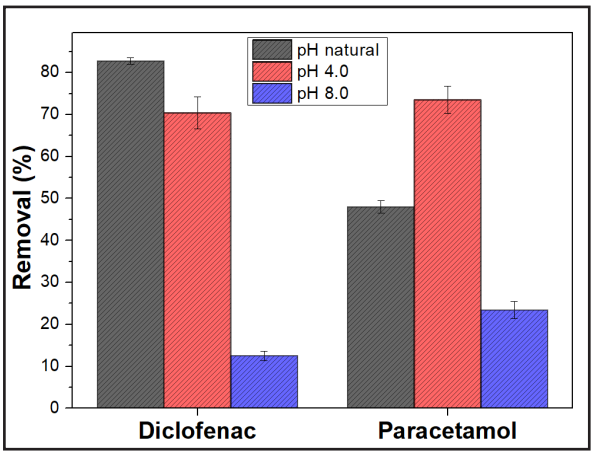

Source: Authors (2024)

The pH of the solution can significantly influence photocatalytic efficiency. As illustrated in Figure 5, the natural pH of diclofenac (pH = 6.5) and the basic pH for paracetamol resulted in the highest photocatalytic activity.

The underlying explanation for the observed behavior is as follows. The pKa values of diclofenac and paracetamol are 4.0 and 9.5 (Borges et al., 2018; Lara-Pérez et al., 2020), respectively, indicating that these molecules predominantly form negatively charged species at pH levels above their respective pKa values. On the other hand, the g-C_3N_4-based photocatalyst has a point of zero charge (pH_{pzc}) in the range of 5.0

to 6.0 (Hernández-Uresti et al., 2016; Jiménez-Salcedo et al., 2022; Zhu et al., 2015). Therefore, at low pH, electrostatic attraction occurs, facilitating interactions between the photocatalyst and the drug molecules. This explains why the intermediate performance observed at pH = 4.0 is favorable, particularly for paracetamol, as it results from the electrostatic attraction between the negatively charged compounds and the positively charged photocatalyst surface.

In the case of diclofenac, at its natural pH (6.5), the photocatalyst's surface charge is close to neutral, leading to enhanced photocatalytic efficiency. Conversely, at pH = 8.0, electrostatic repulsion becomes more pronounced, as both the drug molecules and the photocatalyst surface predominantly carry negative charges, ultimately reducing degradation performance.

3.3 Recycling tests

Figure 6 presents the removal efficiency (%) of diclofenac and paracetamol over multiple reuse cycles of the photocatalyst g-C_3N_4/Nb_2O_5-E. It is observed that as the number of reuses increases, there is a slight decreasing trend in removal efficiency for both compounds, with this decline being more pronounced for diclofenac. In the first reuse cycle (Reuse 01), diclofenac removal remained close to the initial value, indicating that the photocatalyst retains good activity. However, from the second reuse (Reuse 02) onwards, a more noticeable decline in efficiency is observed, which becomes more significant in the third (Reuse 03) and fourth reuse cycles (Reuse 04). This behavior can be attributed to potential photocatalyst deactivation due to the accumulation of byproducts on the surface, structural degradation, or the leaching of active components. For paracetamol, the initial removal efficiency is already lower, possibly due to a lower affinity of this compound for the photocatalyst or slower degradation kinetics. Additionally, the decrease in efficiency with reuse is less pronounced compared to diclofenac, which may indicate that the degradation mechanisms involved are less affected by photocatalyst aging.

Figure 6 – Effect of g-C_3N_4/Nb_2O_5-E Photocatalyst Reuse on the Removal Efficiency of Diclofenac and Paracetamol

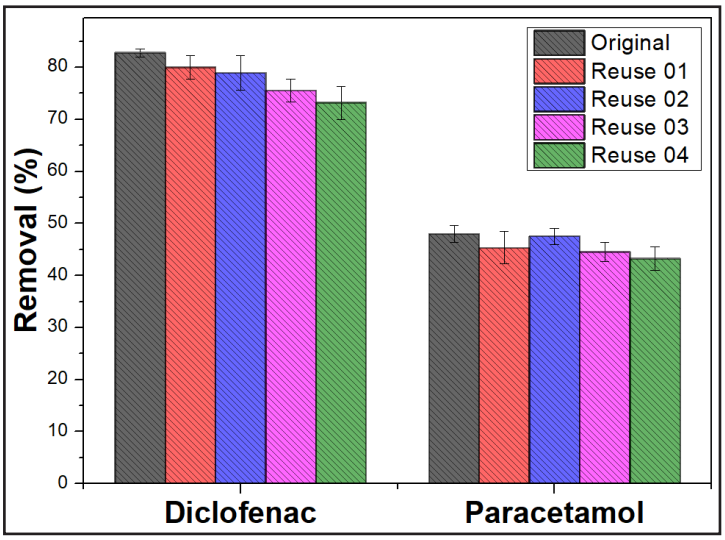

Source: Authors (2024)

3.4 Effect of scavengers

Figure 7 – Effect of scavengers using g-C_3N_4/Nb_2O_5-E on Removal Efficiency of Diclofenac and Paracetamol

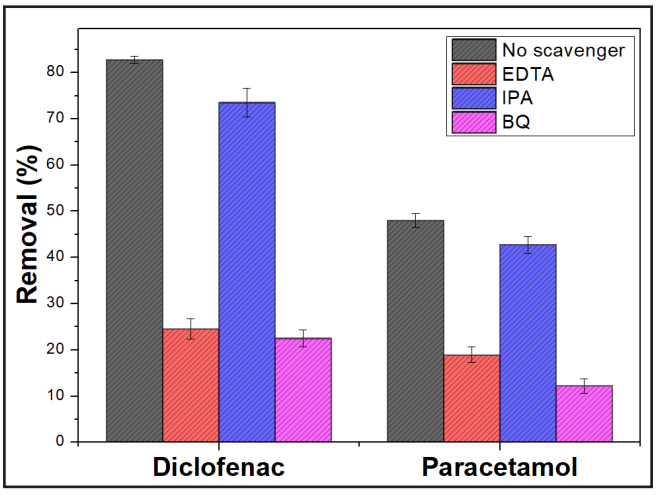

Source: Authors (2024)

To investigate the role of reactive species involved in the photocatalytic degradation of diclofenac and paracetamol, various scavengers were introduced into the reaction system (Figure 7). For the g-C_3N_4/Nb_2O_5-E photocatalyst, a marked

suppression of photocatalytic activity was observed upon the addition of EDTA and BQ, whereas the presence of IPA had a negligible effect on pollutant removal. These findings suggest that photogenerated holes (h^+) and superoxide radicals ($\bullet O_2^-$) are the primary reactive species driving the photocatalytic oxidation, while hydroxyl radicals (•OH) play a less significant role in this process. These results are consistent with previous reports in the literature, in which g-C_3N_4 nanosheets were tested for diclofenac degradation using LED-based light sources (Jiménez-Salcedo et al., 2021).

3.5 Phytotoxicity for lettuce and cucumber seeds

Figure 8 shows the GI values for lettuce and cucumber seeds using the drug paracetamol. For both lettuce and cucumber seeds, the GI (equation 5) for the 20 mg/L paracetamol starting solution showed lower phytotoxicity (higher GI) compared to the control sample. On the other hand, all the samples resulting from the photocatalytic tests after 2h showed lower GI than the control and also lower than paracetamol, thus indicating an increase in phytotoxicity for these seeds.

Considering only the lettuce seeds (Figure 8a), it is important to note that photolysis showed the lowest average GI value among the group of samples, and therefore greater phytotoxicity. This indicates that the samples derived from the photocatalysts, even with low degradation for paracetamol, managed to reduce phytotoxicity compared to the photolysis test. However, it should be noted that the average GI value between all the pairs of samples evaluated (including 20 mg/L paracetamol) were statistically indistinguishable from each other. In this way, the average GI value (77.2%, excluding the control) for lettuce seeds can be taken as a good representation for the group of samples evaluated. Considering only the 04 photocatalysts, the average GI value is 71.2%. Therefore, despite fluctuations in GI values between the samples, the average value found is lower than what the literature typically recognizes as the absence of phytotoxic substances (GI ≥ 80%) (Ravindran et al., 2016; Zucconi, 1981). These results

indicate that, in the context of cucumber seeds, heterogeneous photocatalysis may not be effective in mitigating the phytotoxicity of these seeds.

Similarly to the results for lettuce seeds, the GI for the 20 mg/L paracetamol starting solution showed lower phytotoxicity (higher GI) than the control sample for cucumber seeds (Figure 8b). The average GI for all the routes evaluated with cucumber was 127.8% (excluding the control). However, the GI obtained from the photocatalysis with the g-C_3N_4-E (224.34%) was statistically different from the result obtained with the g-C_3N_4/Nb_2O_5 (70.39%). Thus, excluding the result of the niobium-modified sample, the average GI of the samples was 108.5%. In both cases (averages of 127.8% or 108.5%), the average GI value for cucumber seeds is above the value considered non-phytotoxic (GI ≥ 80%).

Figure 8 – Germination index obtained with lettuce seeds (a) and cucumber seeds (b) for the photocatalysis tests with paracetamol after 120 min of reaction. The bars represent the standard error. The lines above represent the statistical difference between the samples, where * = p ≤ 0.05. The dashed horizontal line represents the average of all the samples (excluding the control)

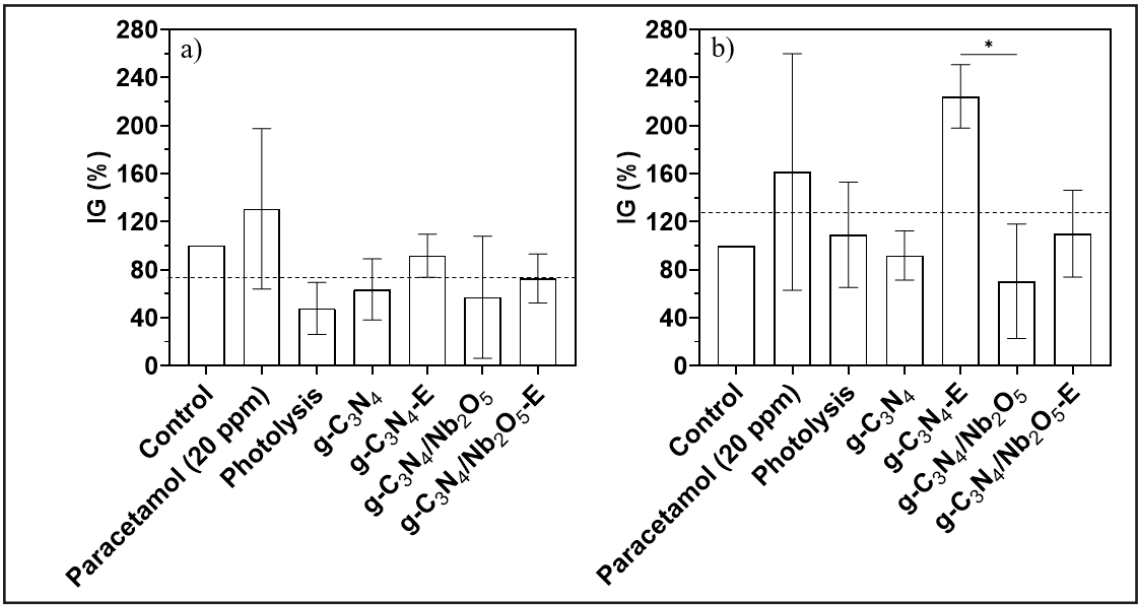

Note: Figures (a) and (b) have been placed between the same limits on the ordinate axis for better comparison
Source: Authors (2024)

It can also be seen (Figure 8b) that the degradation by-products of the samples resulting from the photocatalytic tests after 2 hours tend to have a lower GI compared to paracetamol 20 mg/L and photolysis, the only exception being the g-C_3N_4-E photocatalyst. In other words, it is not possible to say that the photocatalysts were able to reduce phytotoxicity, as the average GI was lower or statistically indistinguishable from the average GI of the photolysis test and paracetamol 20 mg/L. Although the g-C_3N_4-E photocatalyst had the highest GI value, thus suggesting the lowest phytotoxicity of cucumber among the samples, its result was not statistically different from that of paracetamol 20 mg/L or photolysis due to the great variability of the GI around their average.

Figure 9 shows the GI values for lettuce and cucumber seeds exposed to the drug diclofenac. For lettuce seeds (Figure 9a), an increase in GI was observed when comparing the control sample with the initial solution (20 mg/L diclofenac).

Furthermore, when comparing lettuce seeds treated with the initial solution (20 mg/L diclofenac) and those subjected to photolysis, a trend toward increased phytotoxicity (lower GI) was noted. This effect, however, was not evident in the photocatalysis results for paracetamol (Figure 9a), according to the statistical tests. In addition, the photocatalysts g-C_3N_4-E and g-C_3N_4/Nb_2O_5 showed an improvement in GI compared to photolysis, thus suggesting that photocatalytic treatment can help reduce phytotoxicity in these cases, only if compared to tests without photocatalyst. In regard to the g-C_3N_4/Nb_2O_5 specifically, the by-products generated show a significant improvement in phytotoxicity compared to the control, being the only one among the photocatalysts to show this result. In constrast, when comparing the four photocatalysts with each other, there was no statistical difference in the GI value between them.

Therefore, in view of the results shown in Figure 9a, with the exception of the diclofenac degradation by-products generated from the g-C_3N_4/Nb_2O_5, it is not correct to state that the photocatalysts evaluated improved the phytotoxicity of the solution after 2 hours of diclofenac photocatalysis, since none of them was statistically superior to the control sample, the starting solution with 20 mg/L diclofenac and photolysis. Despite

this, the average GI of all the samples evaluated (excluding the control) was 156.5%, while the average GI considering only the 4 photocatalysts was 176.6%, thus suggesting that the photocatalysts do not generate products with worrying phytotoxicity.

A previous study investigated the phytotoxic effects of diclofenac and its photolysis transformation products on *Lactuca sativa* (Murgolo et al., 2018). No inhibition of seed germination was observed during a 24-hour photolysis period. However, slight root growth inhibition was detected in the initial solution. After 4 hours of photolysis, both root and shoot growth were increasingly inhibited, suggesting the formation of more toxic byproducts. Although toxicity decreased at 6 and 24 hours, inhibition levels remained higher than those observed for the original solution, indicating that phototransformation products may be more phytotoxic than the parent molecule. These findings are consistent with the results shown in Figure 9(a), where the germination index (GI) for the photolysis treatment was lower—indicating greater phytotoxicity due to the formation of toxic byproducts—when compared to all the photocatalysts evaluated in the present study. In contrast, when photocatalysis was applied in the same study, no phytotoxic effects were observed throughout the entire treatment period. It is worth noting that the photocatalyst used in that study was based on a hydroxyapatite–TiO_2 composite, which achieved approximately 95% degradation within 24 hours—a significantly longer treatment duration than that evaluated in the present study (120 min.).

In another study (Mohan et al., 2022), the phytotoxicity assessment using *Vigna radiata* seeds showed that water contaminated with diclofenac resulted in poor germination, whereas the effluent treated with the Ni-Zn-F_2O_4 photocatalyst exhibited results comparable to tap water, indicating effective removal of diclofenac and its byproducts, with no significant toxic effects on soil or associated microbiota. However, the germination index (GI) was not measured in this work. Despite this, the g-C_3N_4/Nb_2O_5 sample evaluated in the present study also proved to be promising, as it effectively reduced phytotoxicity.

With regard to cucumber seeds (Figure 9b), the phytotoxicity of diclofenac was slightly lower than that of the control; however, there was no statistically significant

difference between them. In addition, the only statistically significant difference identified in the average GI occurred between the g-C_3N_4 and g-C_3N_4/Nb_2O_5-E.

Figure 9 – Germination index obtained with lettuce seeds (a) and cucumber seeds (b) for the photocatalysis tests with diclofenac after 120 min of reaction. The bars represent the standard error. The lines above represent the statistical difference between the samples, where * = $p \leq 0.05$ and ** = $p \leq 0.01$. The dashed horizontal line represents the average of all the samples (excluding the control)

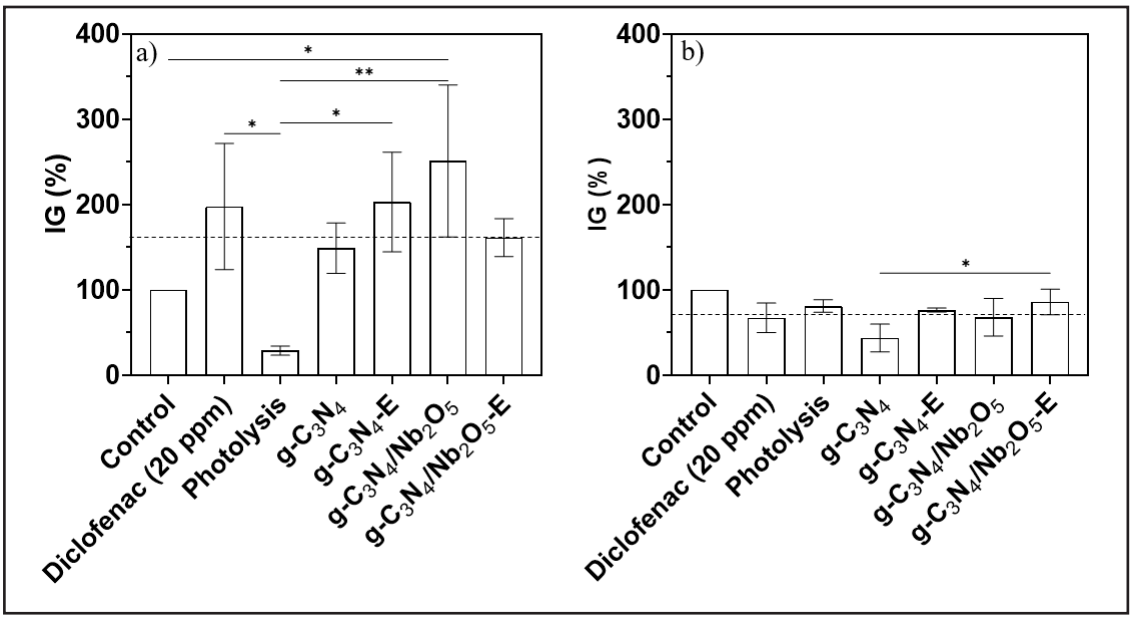

Note: Figures (A) and (B) have been placed between the same limits on the ordinate axis for better comparison
Source: Authors (2024)

No significant differences were observed in the average GI when comparing the samples treated with the photocatalysts to the control group and 20 mg/L diclofenac. This suggests, therefore, that none of the photocatalysts were effective in reducing phytotoxicity to cucumber seeds. For these seeds, the average GI of all the samples evaluated (excluding the control group) was 64.4%. Therefore, in contrast to the results obtained in the paracetamol photocatalysis tests, the by-products resulting from the photodegradation of diclofenac can be considered harmful to the growth of cucumber seeds.

While studies on the phytotoxicity of g-C_3N_4-based photocatalysts are still limited, some researches have shown their potential to reduce phytotoxic effects. For instance, photooxidation of tetracycline hydrochloride using a metal-free carbon nitride functionalized with 8-hydroxyquinoline (Bhoyar et al., 2023) revealed that after treatment with the photocatalyst, the GI for *Cicer arietinum* seed growth reached 92%, a significant improvement compared to the untreated tetracycline solution, which had a GI of just 19%. Another study (Moreira et al., 2019) investigated the photocatalytic degradation of organic micropollutants in urban wastewater under visible light with g-C_3N_4. Their results, based on testing with three plant species (*Sorghum saccharatum*, *Lepidium sativum*, and *Sinapis alba*), demonstrated that photocatalysis did not enhance the toxicity of the treated wastewater.

4 CONCLUSIONS

In summary, this study investigated the effect of exfoliation and the presence of niobium in photocatalysts aimed at the removal of diclofenac and paracetamol under artificial sunlight exposure. Regarding drug degradation, the photocatalysts evaluated demonstrated superior performance compared to photolysis. The average degradation rate of the four photocatalysts studied was higher (71.5%) for diclofenac, being 3.3 times greater than that for paracetamol. The photodegradation results indicate that the exfoliation step and the incorporation of niobium into the photocatalysts lead to better photocatalytic performance. As evidence of this, when comparing with bulk g-C3N4, the photocatalyst g-C_3N_4/Nb_2O_5-E exhibited degradation kinetics values that were 1.5 and 13.8 times greater for diclofenac and paracetamol, respectively. Therefore, exfoliated g-C_3N_4/Nb_2O_5 represents a promising route for the development of more efficient photocatalysts, with potential to expand its application in the degradation of other persistent organic pollutants in wastewater, paving the way for future research in this field.

The results of the photocatalysis tests for paracetamol indicated that cucumber seeds exhibited a higher average germination index (GI) compared to lettuce seeds,

while an inverse trend was noted for diclofenac. Notably, except for the diclofenac degradation by-products generated from the g-C_3N_4/Nb_2O_5 when evaluated with lettuce seeds, none of the other photocatalysts demonstrated statistically significant mean GI values above those of the control and photolysis samples.

Collectively, these findings suggest that simple photolysis may be sufficient for cucumber seeds to maintain acceptable phytotoxicity levels for both drugs, ensuring a GI exceeding 80%. In contrast, lettuce seeds did not show comparable GI performance when subjected to photolysis alone. However, heterogeneous photocatalysis effectively reduced the phytotoxicity of by-products generated with g-C_3N_4-E and g-C_3N_4/Nb_2O_5, but this effect was limited to diclofenac.

ACKNOWLEDGEMENTS

This work was supported by Rio Grande do Sul Research Foundation (FAPERGS Proc. No. 10/2020 21/2551-0000748-6) and *National Council* for Scientific and Technological Development (CNPq, Proc. No. 405411/2023-5).

REFERENCES

Abega, A. V., Marchal, C., Dziurla, M.-A., Dantio, N. C. B., & Robert, D. (2023). Easy three steps gC3N4 exfoliation for excellent photocatalytic activity – An in-depth comparison with conventional approaches. Materials Chemistry and Physics, 304, 127803. https://doi.org/https://doi.org/10.1016/j.matchemphys.2023.127803

Batista, J. A. F. P., C.M., Mendes, J., Silva, M.C.G.S; Escobar, C.C. (2023). Fotocatalsiadores à base de g-C3N4 na degradação de compostos farmacêuticos. In ATENA (Ed.), Soluções inovadoras em engenharia sanitária e ambiental.

Bhoyar, T., Vidyasagar, D., & Umare, S. S. (2023). Mitigating phytotoxicity of tetracycline by metal-free 8-hydroxyquinoline functionalized carbon nitride photocatalyst. Journal of Environmental Sciences, 125, 37-46. https://doi.org/https://doi.org/10.1016/j.jes.2021.10.032

Borges, R. S., Jesus, A. C. S. P. S., Cardoso, L. F., Neri, C. L., Morais, R. B., Barros, V. A., & Silva, A. B. F. d. (2018). Avanços químicos no planejamento e desenvolvimento de derivados do paracetamol. Química Nova, 41.

Carvalho, K. T. G., Nogueira, A. E., Lopes, O. F., Byzynski, G., & Ribeiro, C. (2017). Synthesis of g-C3N4/Nb2O5 heterostructures and their application in the removal of organic pollutants under visible and ultraviolet irradiation. Ceramics International, 43(4), 3521-3530. https://doi.org/https://doi.org/10.1016/j.ceramint.2016.11.063

da Silva, G. T. S. T., Carvalho, K. T. G., Lopes, O. F., & Ribeiro, C. (2017). g-C3N4/Nb2O5 heterostructures tailored by sonochemical synthesis: Enhanced photocatalytic performance in oxidation of emerging pollutants driven by visible radiation. Applied Catalysis B: Environmental, 216, 70-79. https://doi.org/https://doi.org/10.1016/j.apcatb.2017.05.038

Friedmann, D. (2022). A General Overview of Heterogeneous Photocatalysis as a Remediation Technology for Wastewaters Containing Pharmaceutical Compounds. Water, 14(21), 3588. https://www.mdpi.com/2073-4441/14/21/3588

Hassan, F., Backer, S. N., Almanassra, I. W., Ali Atieh, M., Elbahri, M., & Shanableh, A. (2024). Solar-matched S-scheme ZnO/g-C (3)N(4) for visible light-driven paracetamol degradation. Sci Rep, 14(1), 12220. https://doi.org/10.1038/s41598-024-60306-0

Hernández-Uresti, D. B., Vázquez, A., Sanchez-Martinez, D., & Obregón, S. (2016). Performance of the polymeric g-C3N4 photocatalyst through the degradation of pharmaceutical pollutants under UV–vis irradiation. Journal of Photochemistry and Photobiology A: Chemistry, 324, 47-52. https://doi.org/https://doi.org/10.1016/j.jphotochem.2016.01.031

Hong, Y., Li, C., Zhang, G., Meng, Y., Yin, B., Zhao, Y., & Shi, W. (2016). Efficient and stable Nb2O5 modified g-C3N4 photocatalyst for removal of antibiotic pollutant. Chemical Engineering Journal, 299, 74-84. https://doi.org/10.1016/j.cej.2016.04.092

Ines, M., Paolo, P., Roberto, F., & Mohamed, S. (2019). Experimental studies on the effect of using phase change material in a salinity-gradient solar pond under a solar simulator. Solar Energy, 186, 335-346. https://doi.org/https://doi.org/10.1016/j.solener.2019.05.011

Jiang, H., Li, Y., Wang, D., Hong, X., & Liang, B. (2020). Recent Advances in Heteroatom Doped Graphitic Carbon Nitride (g-C3N4) and g-C3N4/Metal Oxide Composite Photocatalysts. Current Organic Chemistry, 24, 673-693. https://doi.org/10.2174/1385272824666200309151648

Jiang, X., Li, J., Fang, J., Gao, L., Cai, W., Li, X., Xu, A., & Ruan, X. (2017). The photocatalytic performance of g-C3N4 from melamine hydrochloride for dyes degradation with peroxymonosulfate. Journal of Photochemistry and Photobiology A: Chemistry, 336, 54-62. https://doi.org/https://doi.org/10.1016/j.jphotochem.2016.12.018

Jiménez-Salcedo, M., Monge, M., & Tena, M. T. (2021). The photocatalytic degradation of sodium diclofenac in different water matrices using g-C3N4 nanosheets: A study of the intermediate by-products and mechanism. Journal of Environmental Chemical Engineering, 9(5), 105827. https://doi.org/https://doi.org/10.1016/j.jece.2021.105827

Jiménez-Salcedo, M., Monge, M., & Tena, M. T. (2022). An organometallic approach for the preparation of Au–TiO2 and Au-g-C3N4 nanohybrids: improving the depletion of paracetamol under visible light. Photochemical & Photobiological Sciences, 21(3), 337-347. https://doi.org/10.1007/s43630-022-00172-9

Karimi, P., Sadani, M., Azarpira, H., Rasolevandi, T., & Sarafraz, M. (2022). Comparative study of energy consumption, kinetic, and performance between conventional and baffled photocatalytic reactor (BPCR) to ofloxacin photo-degradation. Environmental Science and Pollution Research, 29(43), 64914-64923. https://doi.org/10.1007/s11356-022-20066-8

Lara-Pérez, C., Leyva, E., Zermeño, B., Osorio, I., Montalvo, C., & Moctezuma, E. (2020). Photocatalytic degradation of diclofenac sodium salt: adsorption and reaction kinetic studies. Environmental Earth Sciences, 79(11), 277. https://doi.org/10.1007/s12665-020-09017-z

Liu, R., Chen, Z., Yao, Y., Li, Y., Cheema, W. A., Wang, D., & Zhu, S. (2020). Recent advancements in g-C3N4-based photocatalysts for photocatalytic CO2 reduction: a mini review [10.1039/D0RA05779G]. RSC Advances, 10(49), 29408-29418. https://doi.org/10.1039/D0RA05779G

Liu, W., Li, Y., Liu, F., Jiang, W., Zhang, D., & Liang, J. (2019). Visible-light-driven photocatalytic degradation of diclofenac by carbon quantum dots modified porous g-C3N4: Mechanisms, degradation pathway and DFT calculation. Water Research, 151, 8-19. https://doi.org/https://doi.org/10.1016/j.watres.2018.11.084

Mathew, S., Ganguly, P., Kumaravel, V., Bartlett, J., & Pillai, S. C. (2020). Chapter 4 - Solar light-induced photocatalytic degradation of pharmaceuticals in wastewater treatment. In P. Singh, A. Borthakur, P. K. Mishra, & D. Tiwary (Eds.), Nano-Materials as Photocatalysts for Degradation of Environmental Pollutants (pp. 65-78). Elsevier. https://doi.org/https://doi.org/10.1016/B978-0-12-818598-8.00004-3

Mohan, H., Muthukumar Sathya, P., Vadivel, S., Ha, G. H., Oh, H. S., Kim, G., Seralathan, K.-K., & Shin, T. (2022). Highly efficient visible light photocatalysis of Nix Zn1-x Fe2O4 (x= 0, 0.3, 0.7) nanoparticles: Diclofenac degradation mechanism and eco-toxicity. Chemosphere, 301, 134699. https://doi.org/https://doi.org/10.1016/j.chemosphere.2022.134699

Montalvo-Herrera, T., Vallejo-Márquez, J. C., Hernández-Uresti, D. B., & Sánchez-Martínez, D. (2022). Enhanced visible light photoactivity of polymeric g-C3N4 by twice exfoliation in the degradation of acetaminophen and ibuprofen. Journal of Materials Science: Materials in Electronics, 33(20), 16210-16218. https://doi.org/10.1007/s10854-022-08515-z

Moreira, N. F. F., Sampaio, M. J., Ribeiro, A. R., Silva, C. G., Faria, J. L., & Silva, A. M. T. (2019). Metal-free g-C3N4 photocatalysis of organic micropollutants in urban wastewater under visible light. Applied Catalysis B: Environmental, 248, 184-192. https://doi.org/https://doi.org/10.1016/j.apcatb.2019.02.001

Moreno, Y. P., de Escobar, C. C., Skovroinski, E., Weibel, D. E., & dos Santos, J. H. Z. (2022). TiO2/SiO2 dopant-free nanophotocatalysts for highly efficient photocatalytic water splitting: Challenging traditional TiO2-based systems. Journal of Molecular Structure, 1269, 133792. https://doi.org/https://doi.org/10.1016/j.molstruc.2022.133792

Muelas-Ramos, V., Sampaio, M. J., Silva, C. G., Bedia, J., Rodriguez, J. J., Faria, J. L., & Belver, C. (2021). Degradation of diclofenac in water under LED irradiation using combined g-C3N4/NH2-MIL-125 photocatalysts. Journal of Hazardous Materials, 416, 126199. https://doi.org/https://doi.org/10.1016/j.jhazmat.2021.126199

Murgolo, S., Moreira, I. S., Piccirillo, C., Castro, P. M. L., Ventrella, G., Cocozza, C., & Mascolo, G. (2018). Photocatalytic Degradation of Diclofenac by Hydroxyapatite–TiO2 Composite Material: Identification of Transformation Products and Assessment of Toxicity. Materials, 11(9), 1779. https://www.mdpi.com/1996-1944/11/9/1779

Osram, S. M. (2016). More than just light. Solutions in ultraviolet light. 100 Years of Innovation Osram

Papamichail, P., Nannou, C., Giannakoudakis, D. A., Bikiaris, N. D., Papoulia, C., Pavlidou, E., Lambropoulou, D., Samanidou, V., & Deliyanni, E. (2023). Maximization of the photocatalytic degradation of diclofenac using polymeric g-C3N4 by tuning the precursor and the synthetic protocol. Catalysis Today, 418, 114075. https://doi.org/https://doi.org/10.1016/j.cattod.2023.114075

Pizzichetti, R., Reynolds, K., Pablos, C., Casado, C., Moore, E., Stanley, S., & Marugán, J. (2023). Removal of diclofenac by UV-B and UV-C light-emitting diodes (LEDs) driven advanced oxidation processes (AOPs): Wavelength dependence, kinetic modelling and energy consumption. Chemical Engineering Journal, 471, 144520. https://doi.org/https://doi.org/10.1016/j.cej.2023.144520

Puri, M., Gandhi, K., & Kumar, M. S. (2023). Emerging environmental contaminants: A global perspective on policies and regulations. Journal of Environmental Management, 332, 117344. https://doi.org/https://doi.org/10.1016/j.jenvman.2023.117344

Ravindran, B., Kumari, S. K., Stenstrom, T. A., & Bux, F. (2016). Evaluation of phytotoxicity effect on selected crops using treated and untreated wastewater from different configurative domestic wastewater plants. Environ Technol, 37(14), 1782-1789. https://doi.org/10.1080/09593330.2015.1132776

Sigcha-Pallo, C., Peralta-Hernández, J. M., Alulema-Pullupaxi, P., Carrera, P., Fernández, L., Pozo, P., & Espinoza-Montero, P. J. (2022). Photoelectrocatalytic degradation of diclofenac with a boron-doped diamond electrode modified with titanium dioxide as a photoanode. Environmental Research, 212, 113362. https://doi.org/https://doi.org/10.1016/j.envres.2022.113362

Smýkalová, A., Sokolová, B., Foniok, K., Matějka, V., & Praus, P. (2019). Photocatalytic Degradation of Selected Pharmaceuticals Using g-C (3)N(4) and TiO(2) Nanomaterials. Nanomaterials (Basel), 9(9). https://doi.org/10.3390/nano9091194

Torres-Pinto, A., Díez, A. M., Silva, C. G., Faria, J. L., Sanromán, M. Á., Silva, A. M. T., & Pazos, M. (2023). Photoelectrocatalytic degradation of pharmaceuticals promoted by a metal-free g-C3N4 catalyst. Chemical Engineering Journal, 476, 146761. https://doi.org/https://doi.org/10.1016/j.cej.2023.146761

Wang, H., Li, X., Zhao, X., Li, C., Song, X., Zhang, P., Huo, P., & Li, X. (2022). A review on heterogeneous photocatalysis for environmental remediation: From semiconductors to modification strategies. Chinese Journal of Catalysis, 43(2), 178-214. https://doi.org/https://doi.org/10.1016/S1872-2067(21)63910-4

Zhang, M., Yang, Y., An, X., Zhao, J., Bao, Y., & Hou, L.-a. (2022). Exfoliation method matters: The microstructure-dependent photoactivity of g-C3N4 nanosheets for water purification. Journal of Hazardous Materials, 424, 127424. https://doi.org/https://doi.org/10.1016/j.jhazmat.2021.127424

Zheng, Q., Durkin, D. P., Elenewski, J. E., Sun, Y., Banek, N. A., Hua, L., Chen, H., Wagner, M. J., Zhang, W., & Shuai, D. (2016). Visible-Light-Responsive Graphitic Carbon Nitride: Rational Design and Photocatalytic Applications for Water Treatment. Environmental Science & Technology, 50(23), 12938-12948. https://doi.org/10.1021/acs.est.6b02579

Zhou, S., Di Paolo, C., Wu, X., Shao, Y., Seiler, T.-B., & Hollert, H. (2019). Optimization of screening-level risk assessment and priority selection of emerging pollutants – The case of pharmaceuticals in European surface waters. Environment International, 128, 1-10. https://doi.org/https://doi.org/10.1016/j.envint.2019.04.034

Zhu, B., Xia, P., Ho, W., & Yu, J. (2015). Isoelectric point and adsorption activity of porous g-C3N4. Applied Surface Science, 344, 188-195. https://doi.org/https://doi.org/10.1016/j.apsusc.2015.03.086

Zucconi, F. (1981). Evaluating Toxicity of Immature Compost. Biocycle, 22, 54-57.

Authorship contributions

1 – Julia Mendes

Currently pursuing a Master's degree in Hydraulic and Sanitary Engineering at the USP.
https://orcid.org/0009-0008-8808-5438 • mndsjuliax@gmail.com
Contribution: conceptualization, data curation, formal analysis, investigation, methodology, writing – original draft, writing – review & editing

2 – José André Ferreira Batista

Master's degree in Environmental Sciences from the UFPEL.
https://orcid.org/0009-0004-0414-5749 • andrebatista1975@gmail.com
Contribution: data curation, investigation, methodology, writing – review & editing

3 – Maria Carolina Gomes Silva e Silva

Currently pursuing a degree in Environmental and Sanitary Engineering at the UFPEL.
https://orcid.org/0009-0002-4976-2869 • emariacarolinagssilva@gmail.com
Contribution: data curation, investigation, writing – original draft

4 – Willian Cézar Nadaleti

PhD in Environmental Engineering from the UFSC.
https://orcid.org/0000-0002-4727-4127 • willian.nadaleti@ufpel.edu.br
Contribution: formal analysis, investigation, writing – original draft

5 – Cátia Fernandes Leite

PhD in Materials Science and Engineering from the UFPEL.
https://orcid.org/0000-0002-5415-9709 • cfleite@ufpel.edu.br
Contribution: formal analysis,methodology, writing – original draft

6 – Priscila Martta Rodrigues

PhD in Mechanical Engineering from the UNISINOS.
https://orcid.org/0000-0002-1346-1418 • priscilamartta@edu.unisinos.br
Contribution: data curation, formal analysis, investigation, writing – original dratf, writing – review & editing

7 – Cícero Coelho de Escobar

PhD in Chemical Engineering from the UFRGS.
https://orcid.org/0000-0002-6248-9222 • cicero.escobar@ufpel.edu.br
Contribution: funding acquisition, supervision

How to quote this article

Mendes, J., Batista, J. A. F., Silva e Silva, M. C. G., Nadaleti, W. C., Leite, C. F., Rodrigues, P. M.,& Escobar, C. C. de. (2026). Photocatalytic degradation and phytotoxicity assessment of diclofenac and paracetamol using exfoliated g-C_3N_4/Nb_2O_5 under sunlight. *Ciência E Natura*, 48, e85500. DOI: 10.5902/2179460X85500. Available in: https://doi.org/10.5902/2179460X89084